Electronic Supporting Information

Fluorescence Detection of Spermine and Spermidine Using a Poly-Carboxylate Receptor and Ensemble-based Formalin Sensing in real samples

Sulekha Kumari Pandit and Gopal Das*

Department of Chemistry, Indian Institute of Technology Guwahati, Assam, 781039, India

E-mail: gdas@iitg.ac.in

General Methods and Materials

All reagents, starting materials, solvents, and protein samples were procured from commercial sources and used without further purification. The solvents used were HPLC grade. For N.M.R. analyses, deuterated solvent [$(CD_3)_2SO$] was purchased from Sigma-Aldrich. Chemical shifts of NMR were recorded using a BRUKER-400 MHz and a BRUKER-600 MHz instrument and reported on a scale in parts per million (ppm). Spin multiplicities from ^1H NMR spectra were described using the following abbreviations: s = singlet; d = doublet; t = triplet; m = multiplet. The absorption and emission spectral studies were measured in a Perkin-Elmer Lamda-25. UV-Vis spectrophotometer and Horiba Fluoromax-4 spectrofluorometer respectively. Recording of UV-vis spectra was done in 10 mm path-length quartz cuvettes in the range of 300-600 nm wavelength, while fluorescence measurement was done using a 10 mm path-length quartz cuvette with a slit width of 5 nm at 25 °C.

IR spectra with 4000-400 cm^{-1} range were collected using a Perkin Elmer-Spectrum AT-IR spectrometer.

High-resolution mass spectrometry was carried out on Agilent 1100/1200/1260/1290 LC Q-ToF mass spectrometer.

Fluorescence spectral studies

TP and TPC's stock solutions were made in DMSO at a concentration of 5×10^{-3} M and diluted to 10 μM. Biogenic amines (0.05 M) solution was produced in water, for aqueous medium selectivity investigations and diluted suitably for subsequent experiments. In fluorescence studies, a quartz optical cell with a path length of 10 mm was filled with a 2.0 mL solution of TP/TPC, and biogenic amine, anions, and cations of stock solutions were gradually added with the aid of a micropipette. Excitation was given at 365 nm. For standard selectivity and titration experiments, emission was measured from 375 to 600 nm. Within 5 sec of adding the external ions, spectral data were collected. All experiments were conducted in 100% aq media.

Field Emission Scanning Electron Microscope

Zeiss, Model: Gemini 300 and Sigma 300 were used to characterize the topographical and morphological details. Imaging studies were conducted separately with a solution of 20 μM by drop-casting (2 μl) on glass plates covered with Al-foil.

Detection Limit

From the fluorescence titration profile, the detection limits were obtained. In this calculation, to obtain the standard deviation(σ) of blank measurement, the fluorescence emission spectrum of the probe as well as the ensemble were measured 10 times. In the case of slope determination, the ratio of the fluorescence emission at a certain wavelength was plotted against the concentration of the guest analyte. The equation used for deducting the detection limit is as follows:

$$\frac{3\sigma}{K} = Detection\ Limit$$

Where, σ = standard deviation of blank measurement, k = slope between the ratio of fluorescence emission vs corresponding guest concentration.

Dynamic light scattering studies

The particle sizes of TP and TP+analyte were measured by dynamic light scattering (DLS) experiments on the Litesizer DLS 500 instrument with a focus position of 0.9 mm. The samples and the background were measured at room temperature (25 °C). DLS experiments were carried out with optically clear solutions of 10 μM to observe the change in the particle size upon the addition of an analyte. The solution was freshly prepared for the measurements.

Estimation of the Apparent Binding Constant

From the fluorescence titration profile, the binding constant was accessed utilizing the Benesi−Hildebrand (B−H) plot (Equation 2).

$$\frac{1}{K(I_{max} - I_0)C} + \frac{1}{I_{max} - I_0} = \frac{1}{I - I_0} \quad \text{.....(2)}$$

Multiplying both sides with $(I_{max} - I_0)$

$$\frac{(I_{max} - I_0)}{I - I_0} = \frac{1}{K[C]} + 1$$

I_0 is the emission intensity of TP at maximum (λ = 440 nm), and I is the recorded emission intensity at that particular wavelength in the presence of a specific concentration of the analyte (C). I_{max} is the maximum emission intensity value obtained at λ = 440 nm during titration with varying analyte concentrations. K is the apparent binding constant (M^{-1}) and was determined from the linear plot's slope.

Measurement of fluorescence lifetime

Fluorescence lifetimes were evaluated utilizing the time-correlated single-photon counting (TCSPC) method in the Edinburgh Instrument Life-Spec II spectrometer. The samples (TP and TP+Spermine/Spermidine) were excited at 375 nm laser keeping the emission wavelength at 440 nm using a pulsed diode laser. The fluorescence decays were surveyed by the re-convolution method using the FAST software provided by Edinburgh Instruments.

$$\tau_{av} = \frac{f_1\tau_1 + f_2\tau_2}{f_1 + f_2} \ldots\ldots\ldots for\ bi - exponential\ decay$$

The weights f_1 and f_2 correspond to the relative amplitudes of the decay components, and the lifetimes τ_1 and τ_2 correspond to the decay times.

Quantum Yield Calculation

The quantum yield (Φ) was measured by comparing the integrated photoluminescence intensities and the absorbance values with the reference quinine sulfate (QS). The quinine sulfate (literature Φ = 0.54) was dissolved in 0.1 M H_2SO_4 (refractive index (η) of 1.33) and the receptors were dissolved in distilled water (η = 1.33). Where Φ is the quantum yield, I is the measured integrated emission intensity, and η is the refractive index. A_R and A represent the absorbance at the excitation wavelength of 340 nm of the quinine sulfate and receptors respectively. The subscript R refers to the reference fluorophore of known quantum yield.

$$\Phi = \Phi_R \times \frac{I}{I_R} \times \frac{A_R}{A} \times \frac{\eta^2}{\eta_R^2}$$

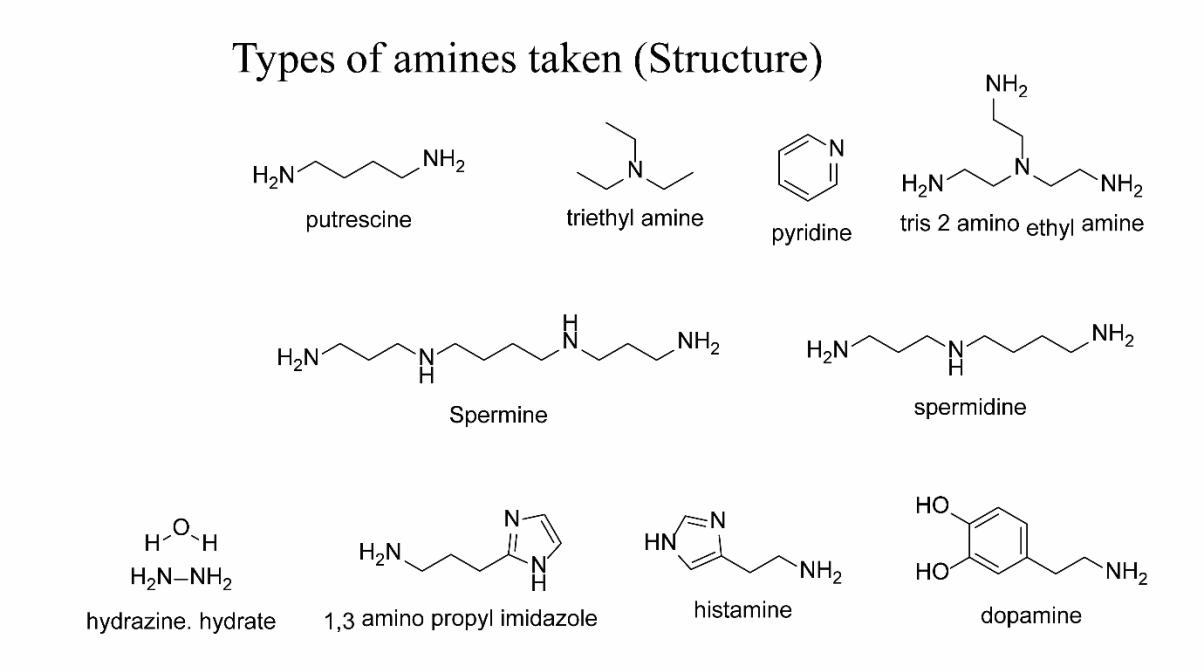

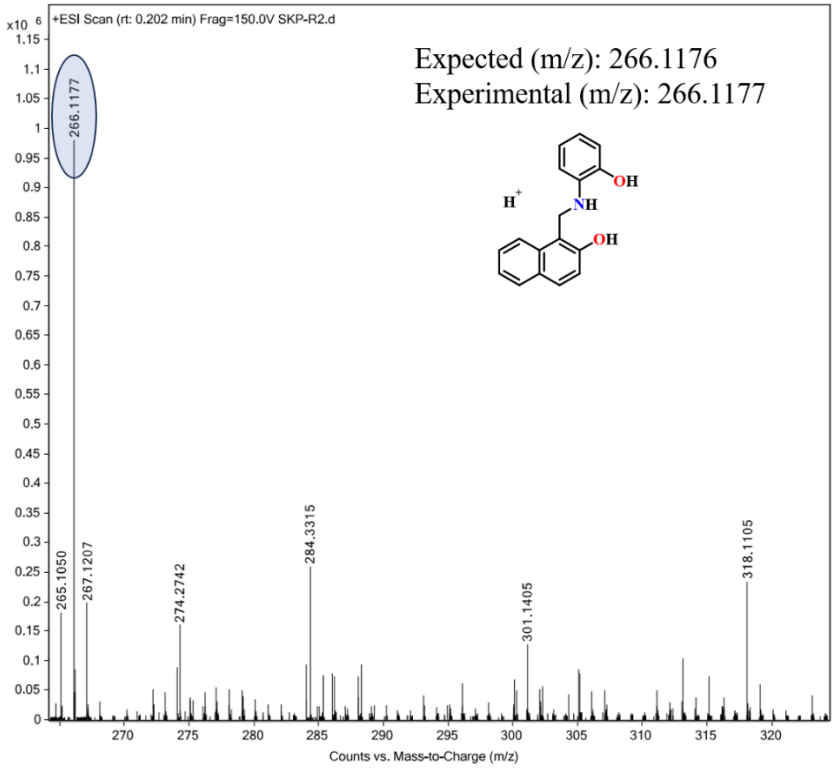

Fig S1 HRMS of SR in positive ionization mode.

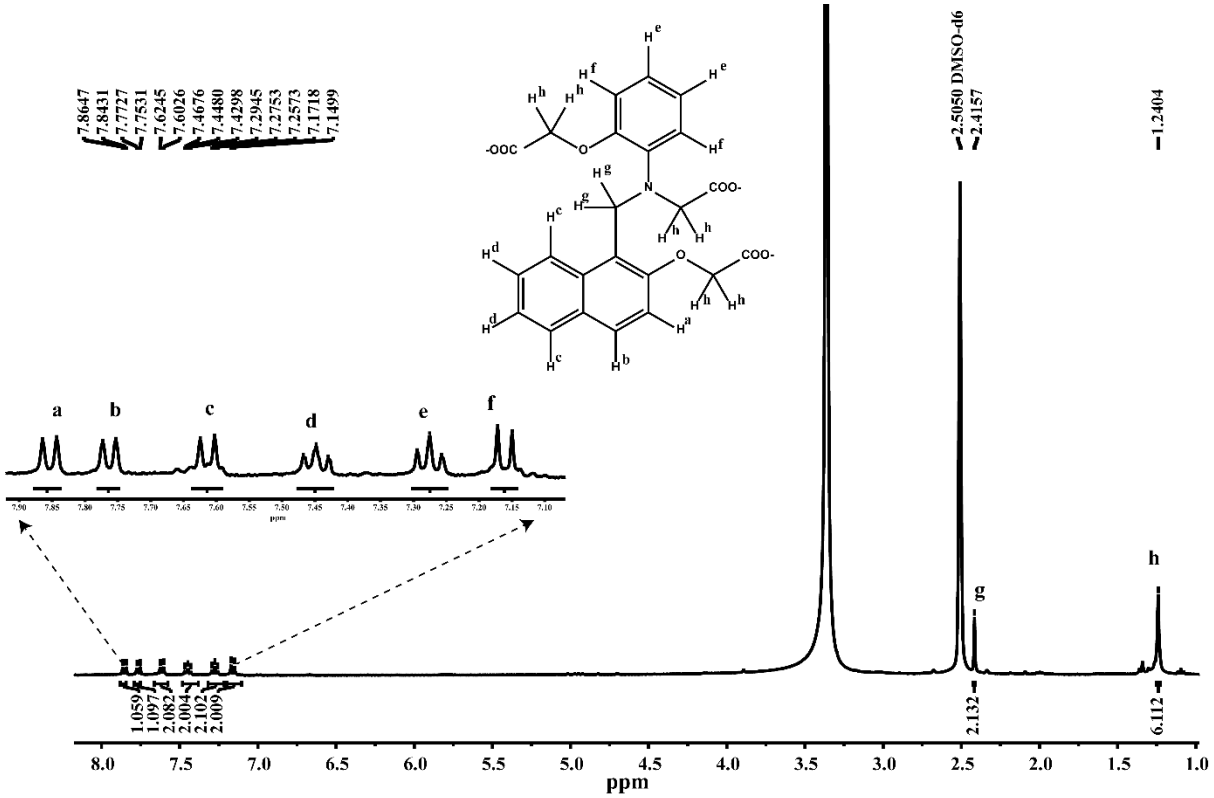

Fig S2 ^{1}H NMR of TP (DMSO-d_6, Room Temperature).

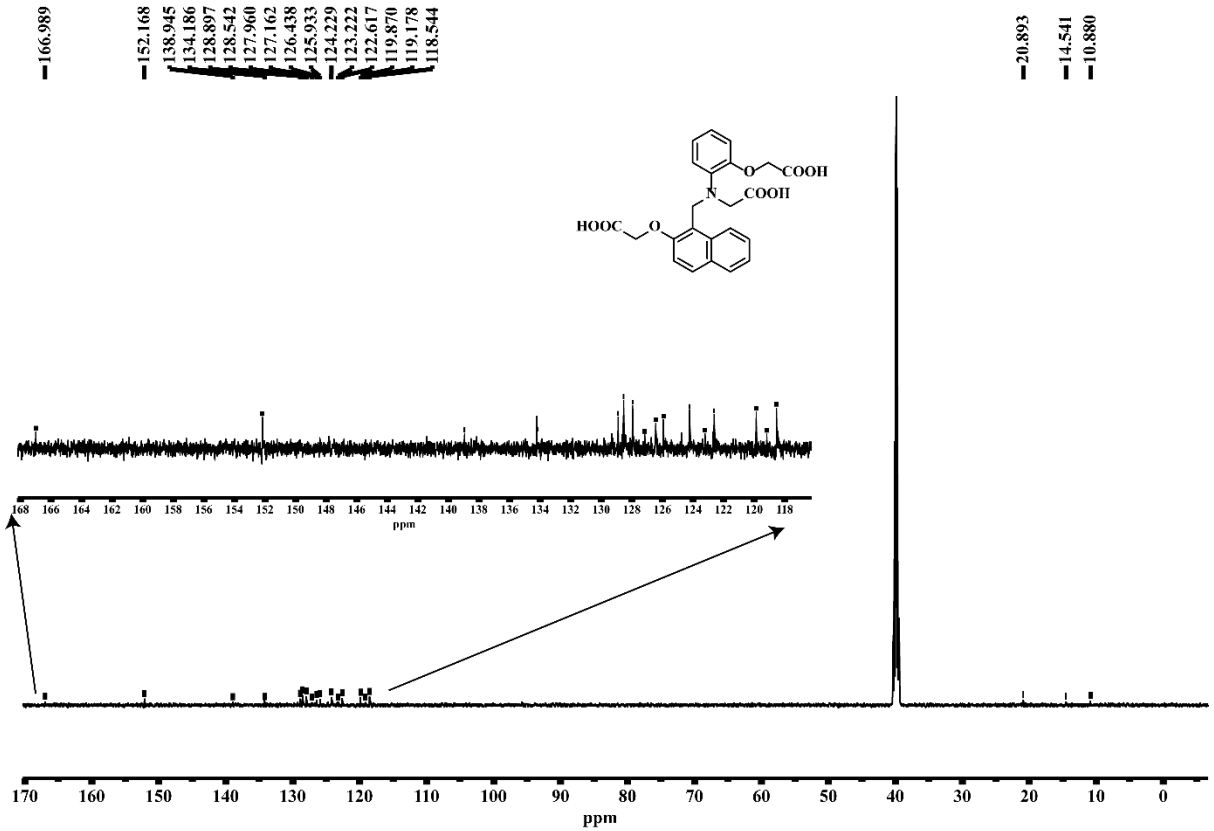

Fig S3 ^{13}C NMR of TP (DMSO-d_6, Room Temperature).

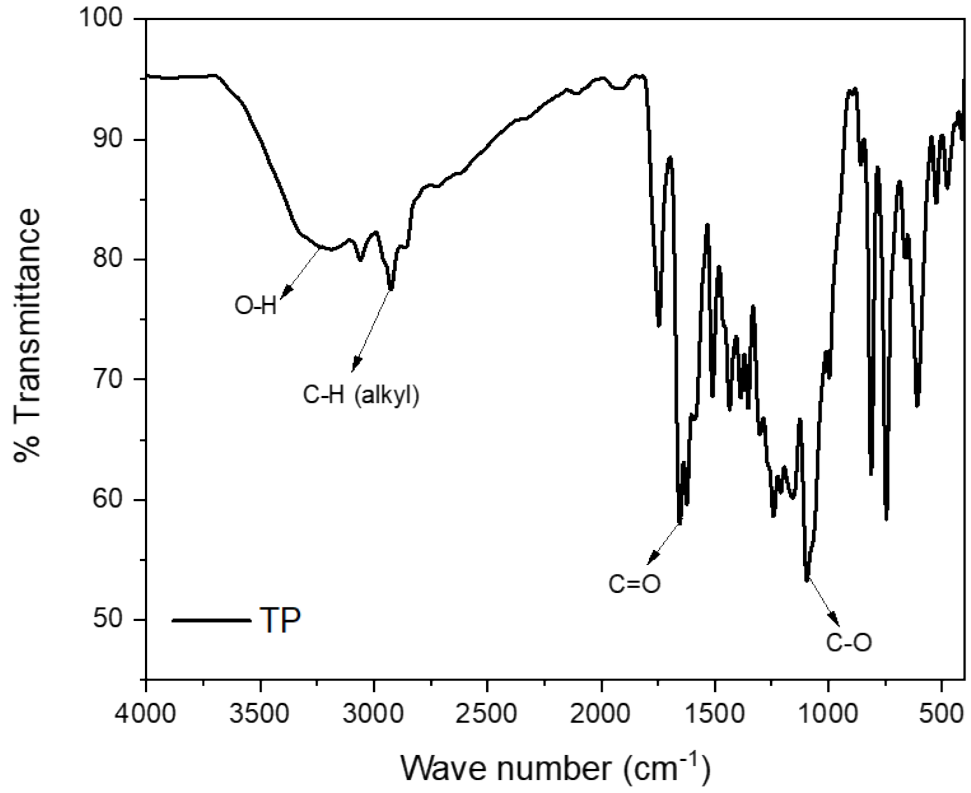

Fig S4 AT-IR Spectra of TP.

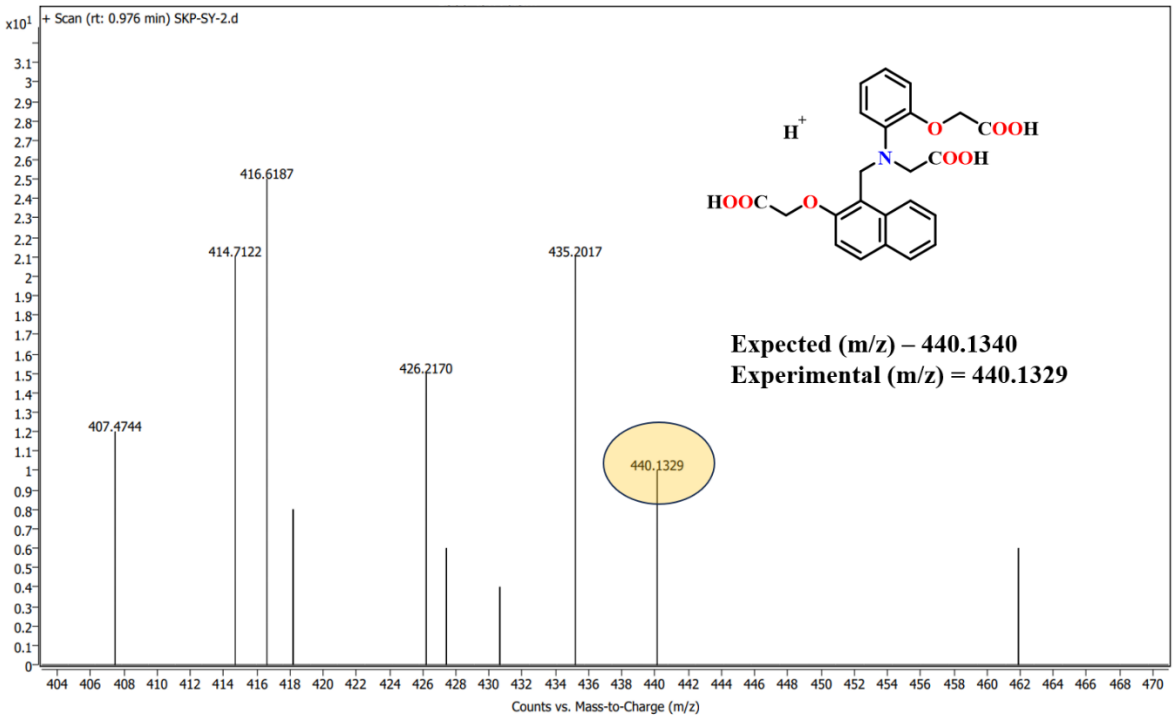

Fig S5 HRMS of TP in positive ionization mode.

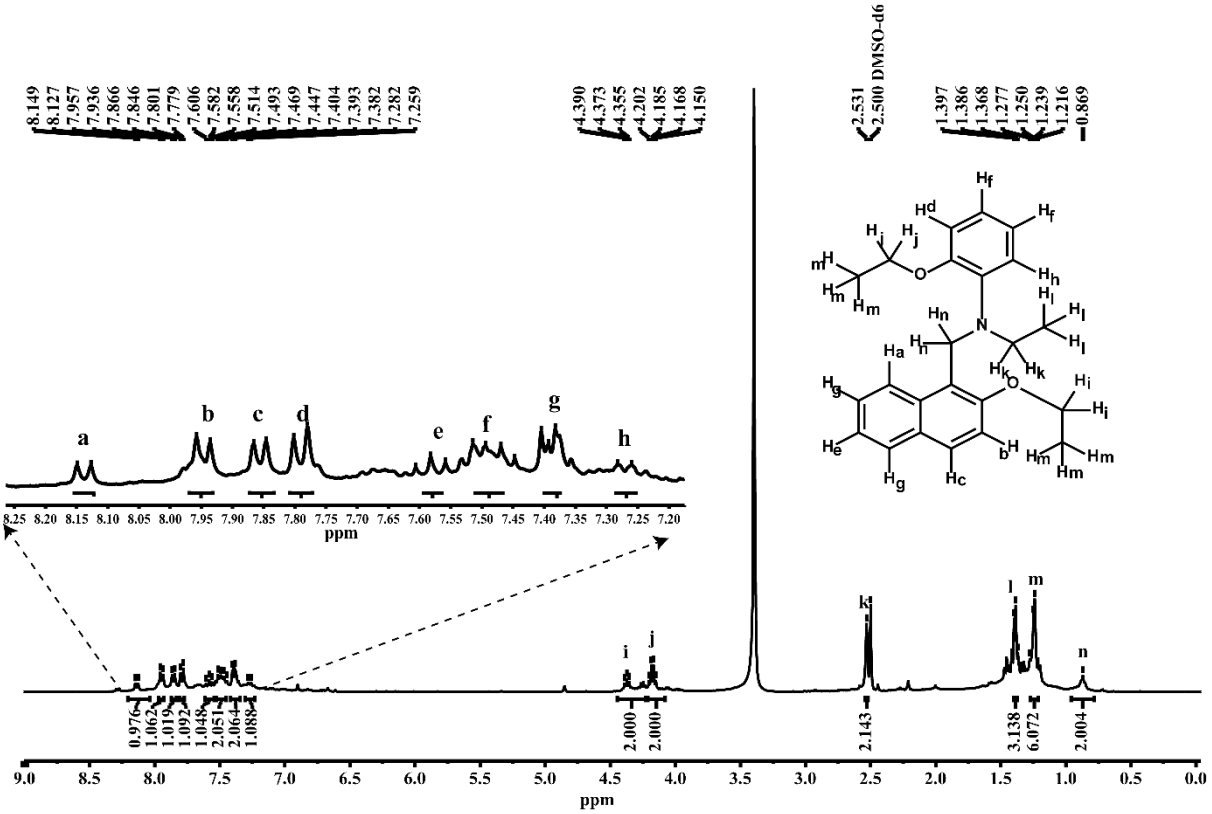

Fig S6 ^{1}H NMR of TPC (DMSO-d_6, Room Temperature).

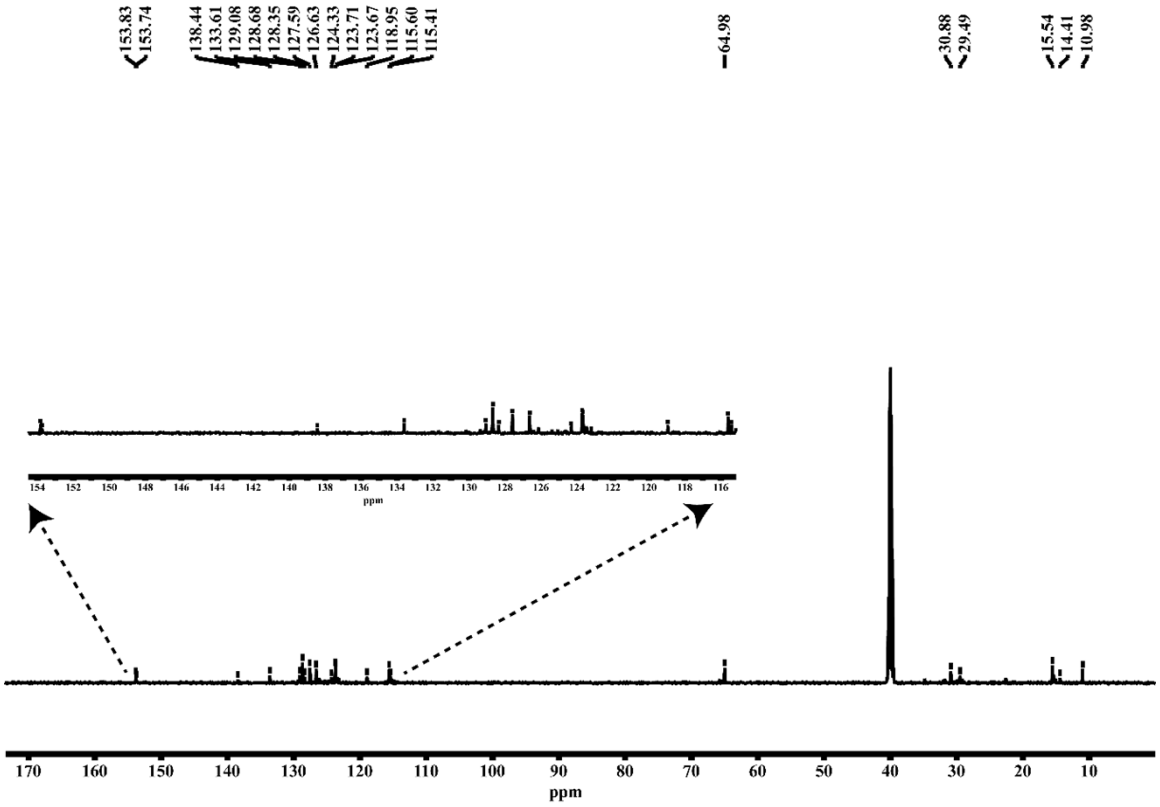

Fig S7 ^{13}C NMR of TP (DMSO-d_6, Room Temperature).

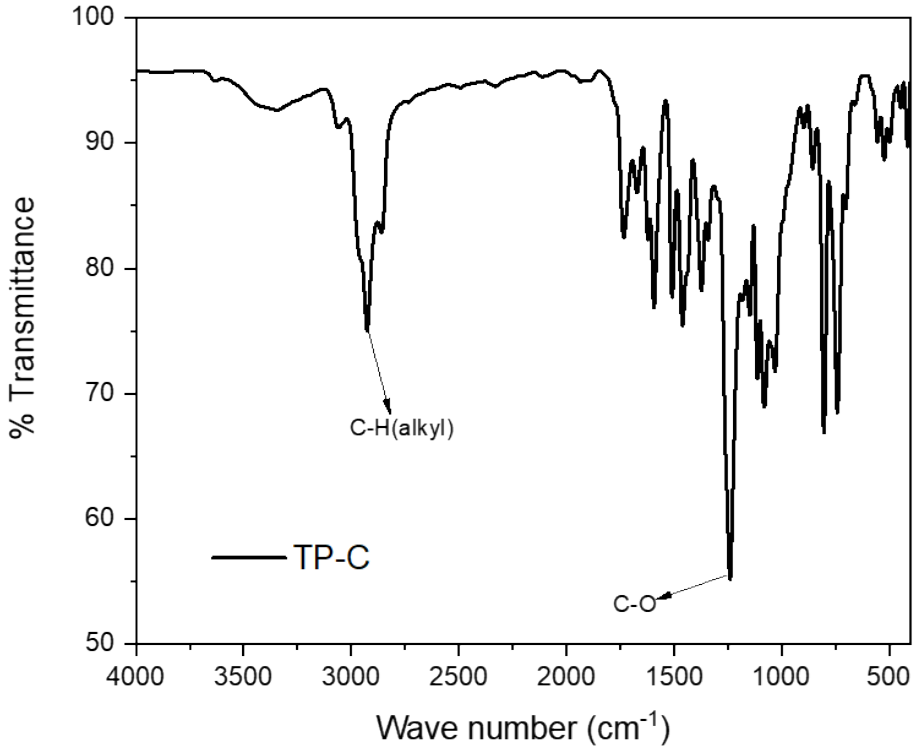

Fig S8 AT-IR Spectra of TP.

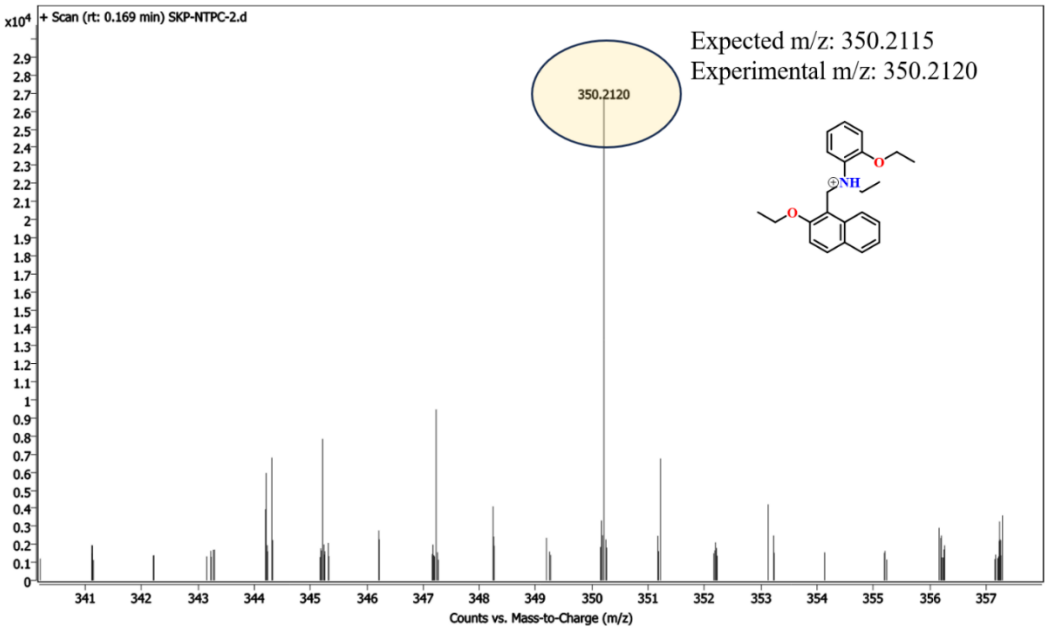

Fig S9 HRMS of TPC in positive ionization mode.

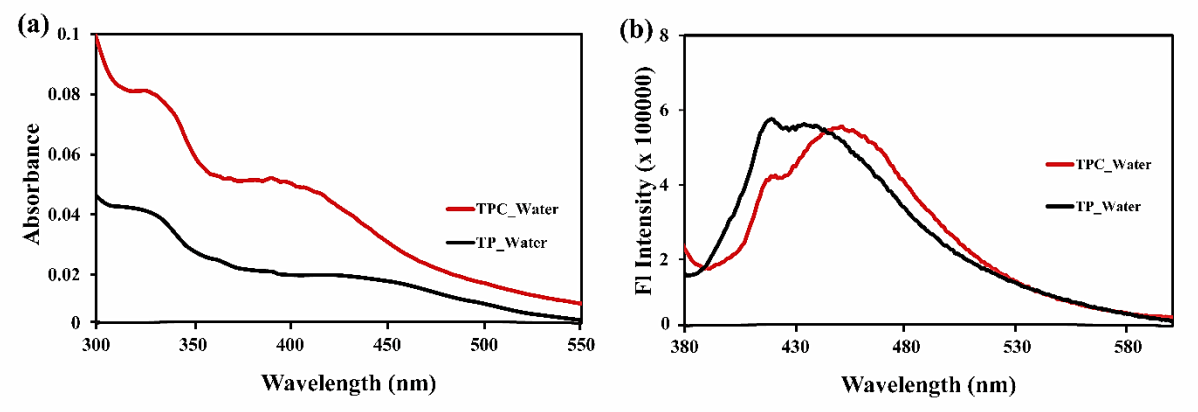

Fig S10 (a) Absorption spectra of TP and TPC in water (b) Emission spectra of TP and TPC in water.

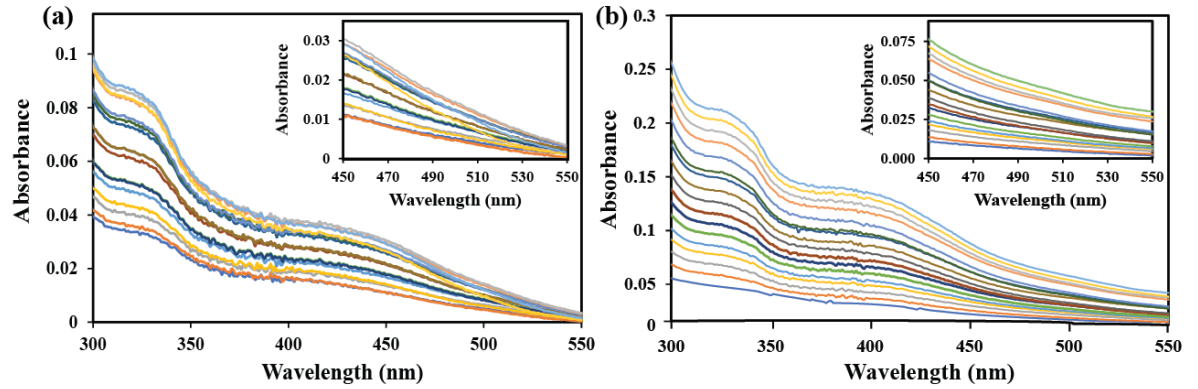

Fig S11 Concentration Vs absorbance plot for (a) TP and (b) TPC (Inset: Upsurging of baseline with an increase in conc).

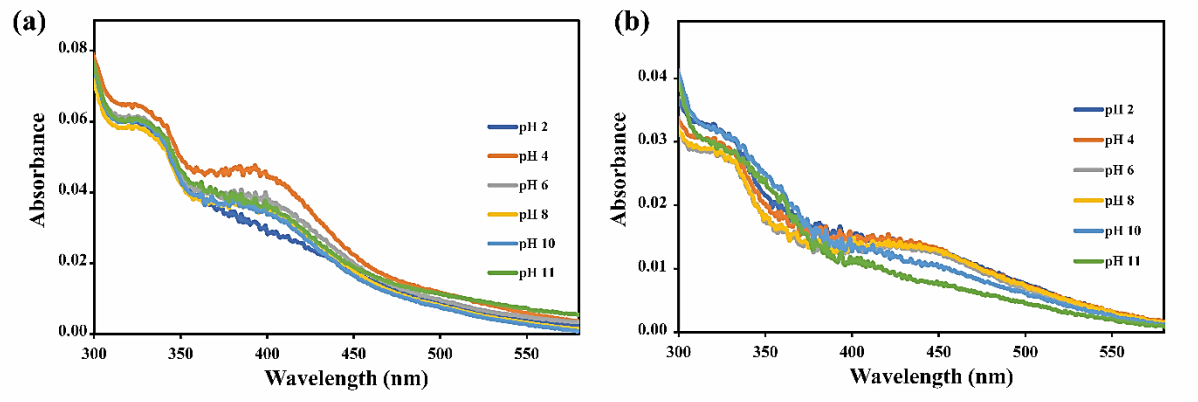

Fig S12 Absorption spectra oat different pH (a) TP and (b) TPC.

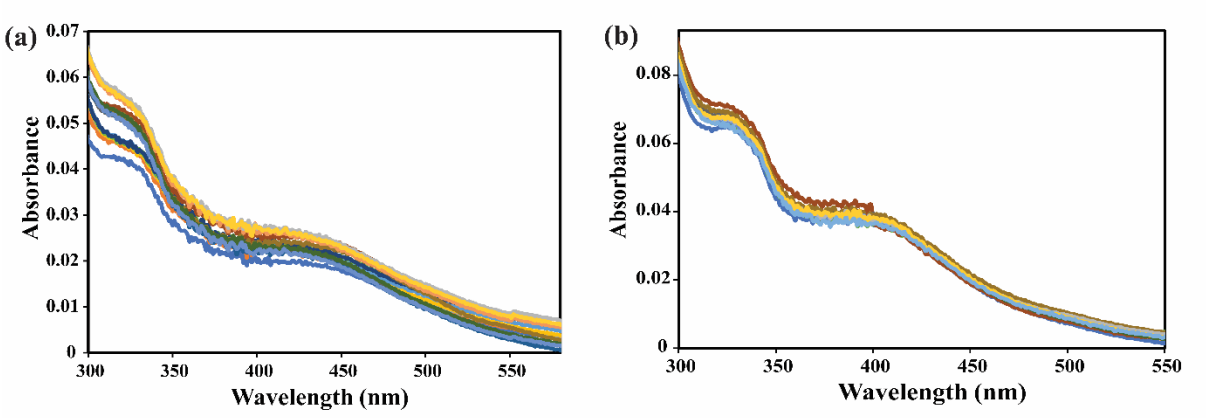

Fig S13 Absorption spectra with various analytes in aqueous solvent (a) TP (b) TPC.

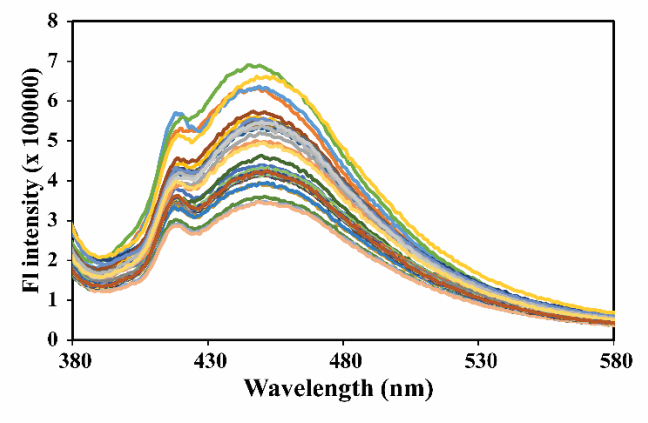

Fig S14 Emission spectra of TPC with various anionic analytes (5×10^{-2} M) in 100% aqueous environment.

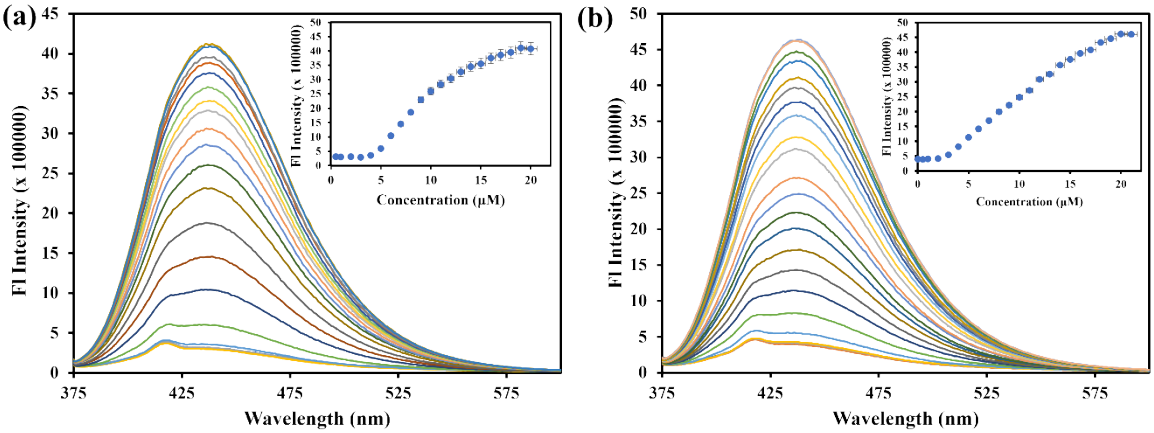

Fig S15 (a) Fluorescence emission titration on incremental addition of spermidine to TP [Inset: Emission intensity at 440 nm as a function of concentration of spermidine added] (b) Fluorescence emission titration on incremental addition of spermine to TP [Inset: Emission intensity at 440 nm as a function of concentration of spermine added].

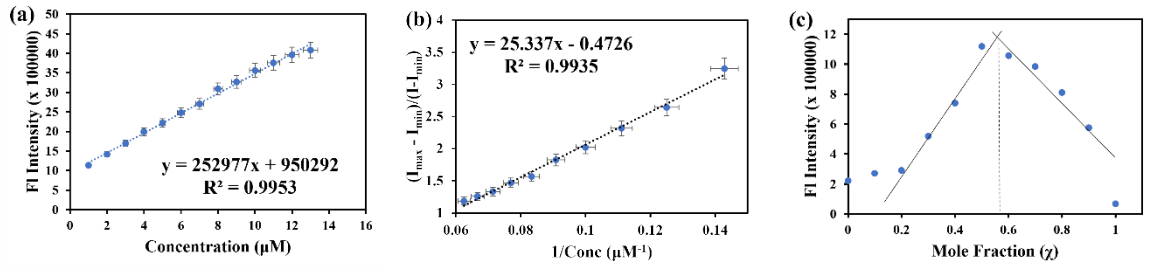

Fig S16 (a) Linear relationship between the concentration of spermine for the detection limit (LOD) calculation (b) B-H plot for determination of binding constant (c) Job's plot showing 1:1 complex formation

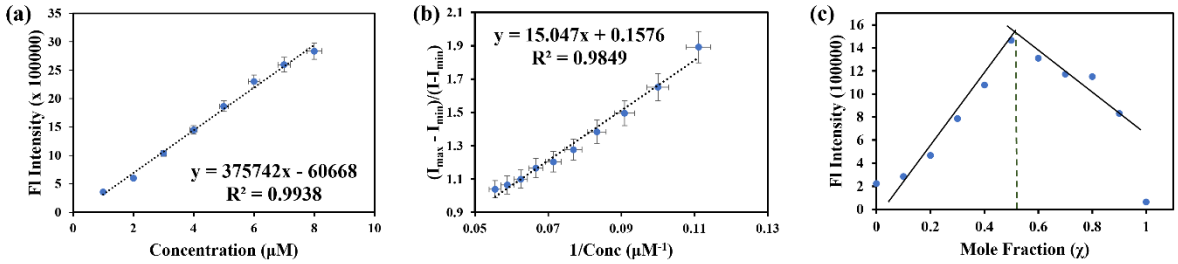

Fig S17 (a) Linear relationship between the concentration of spermidine for the detection limit (LOD) calculation (b) B-H plot for determination of binding constant (c) Job's plot showing 1:1 complex formation.

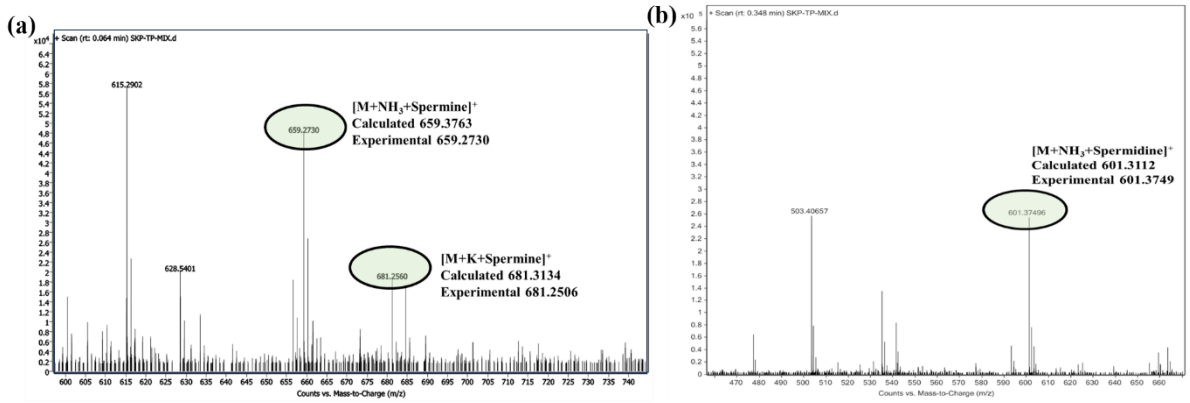

Fig S18 Mass Spectrometry of 1:1 binding.

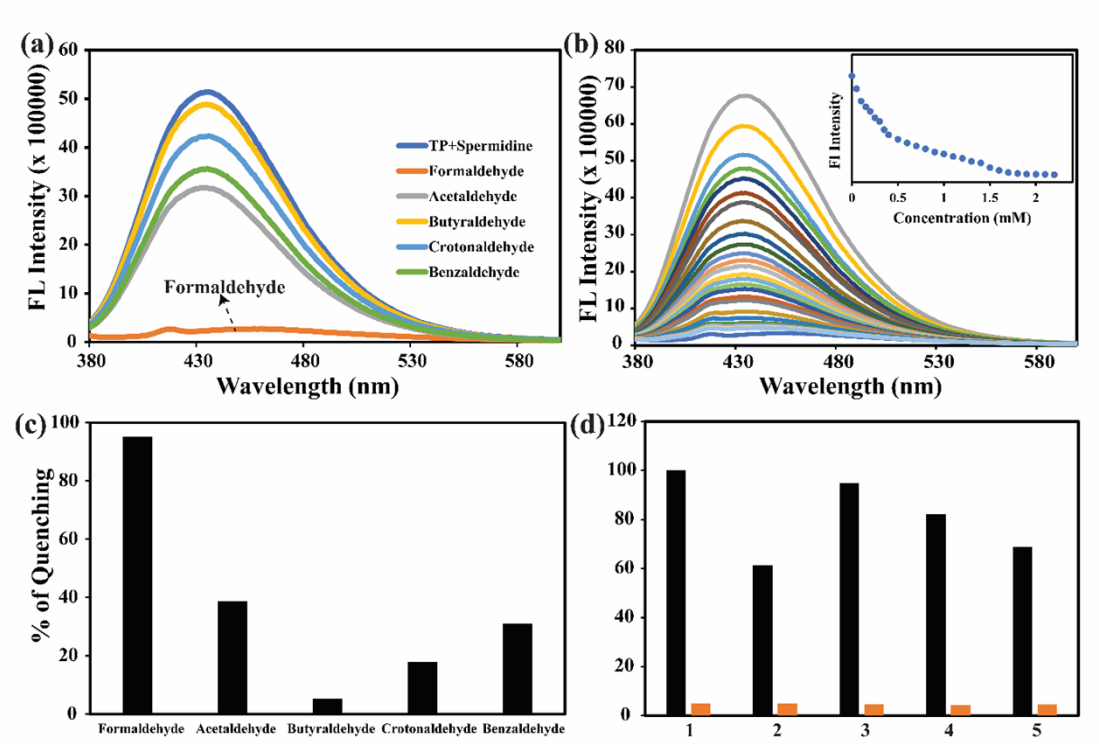

Fig S19 (b) TP⊂Spermidine Ensemble

Sensing of formalin in the presence among other aldehydes in the presence of TP⊂Spermidine Ensemble (b) Fluorescence emission titration on incremental addition of HCHO to TP⊂Spermidine Ensemble [Inset: Emission intensity at 440 nm as a function of the concentration of HCHO added] (c) Bar Graph representing percentage of quenching in presence of different aldehyde for TP⊂Spermidine Ensemble (d) Interference in presence of different aldehyde [Black=TP⊂Spermidine + other aldehyde, Orange=TP⊂Spermidine + other aldehyde+HCHO, 1= Formaldehyde, 2=acetaldehyde, 3=Butyraldehyde, 4=Crotonaldehyde, 5=Benzaldehyde]

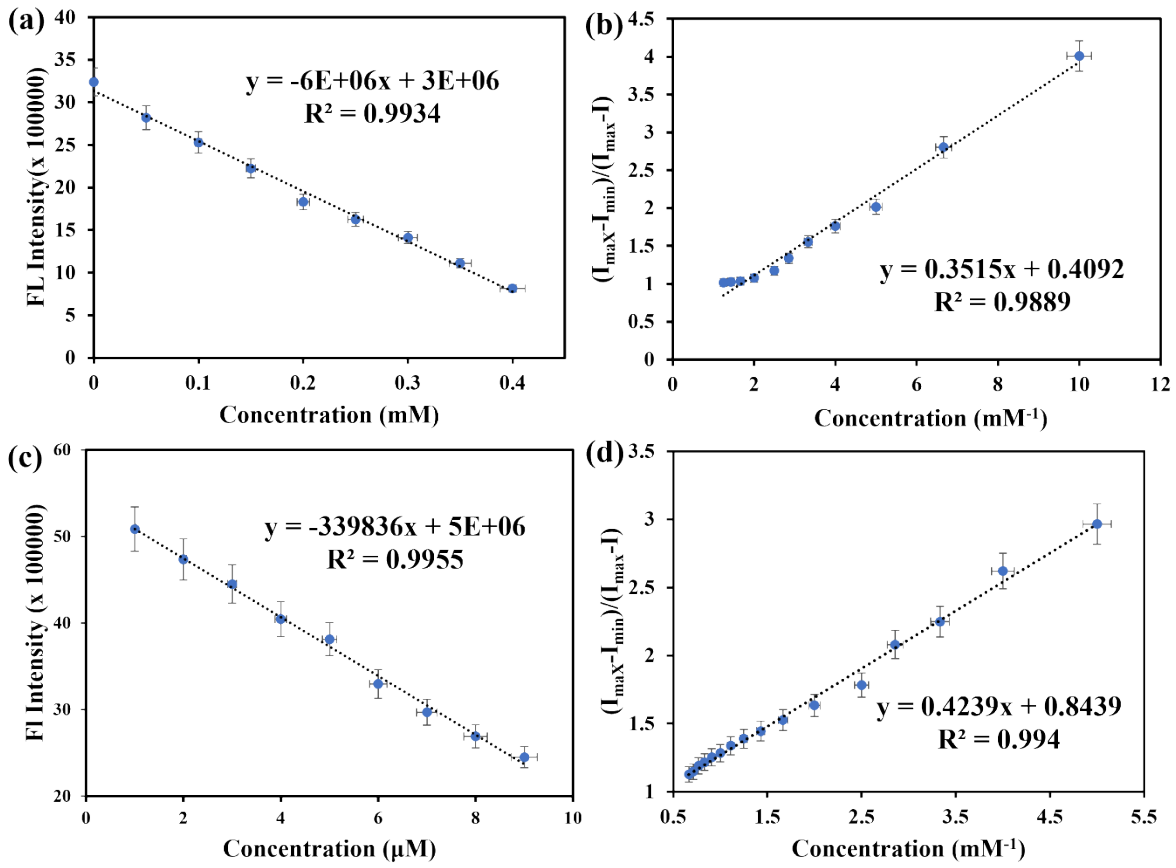

Fig S20 TP⊂Spermine Ensemble (a) Linear relationship between the concentration of Formalin for the detection limit (LOD) calculation (b) B-H plot for determination of binding constant. TP⊂Spermidine Ensemble (c) Linear relationship between the concentration of Formalin for the detection limit (LOD) calculation (d) B-H plot for determination of binding constant.

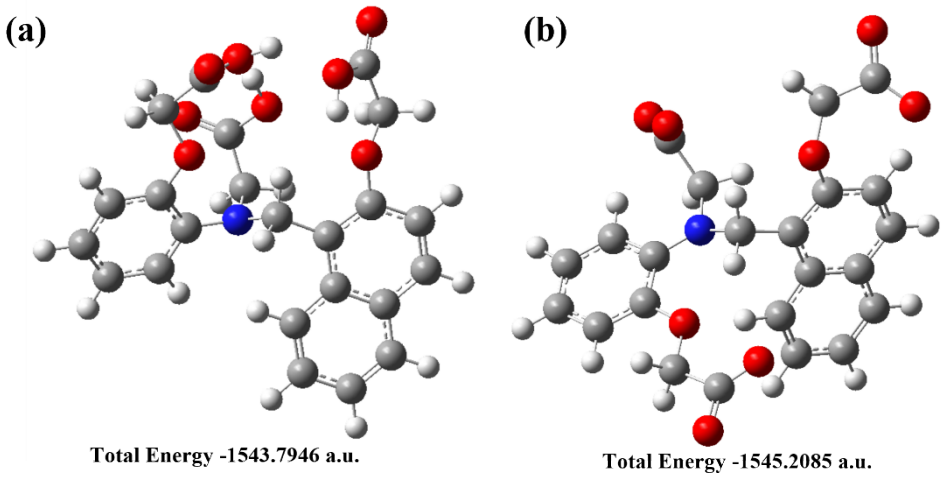

Fig S21 DFT computed optimized geometry of (a) TP and (b) Deprotonated TP in water using the B3LYP/6-31 G level of theory (CPCM model).

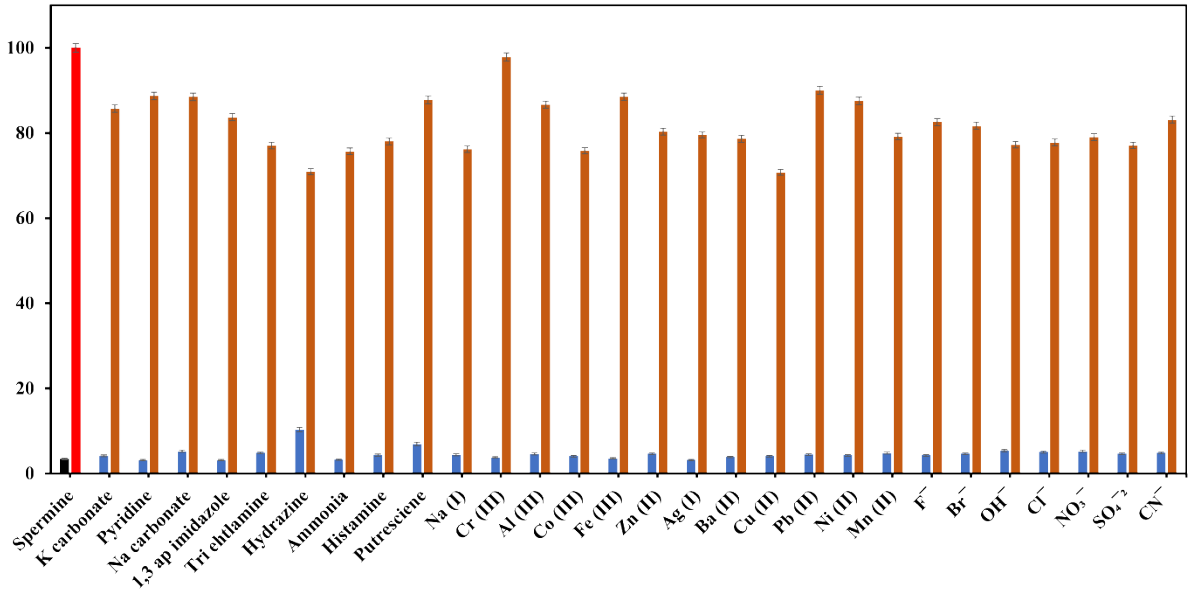

Fig S21 The % fluorescence intensity contrast bars to investigate the interference effect of other similar molecules and inorganic species to test objects on the detection ability of TP for Spermine (SPM). TP-black, Red-TP+SPM, Blue=TP+analytes, Orange=TP+analytes+SPM

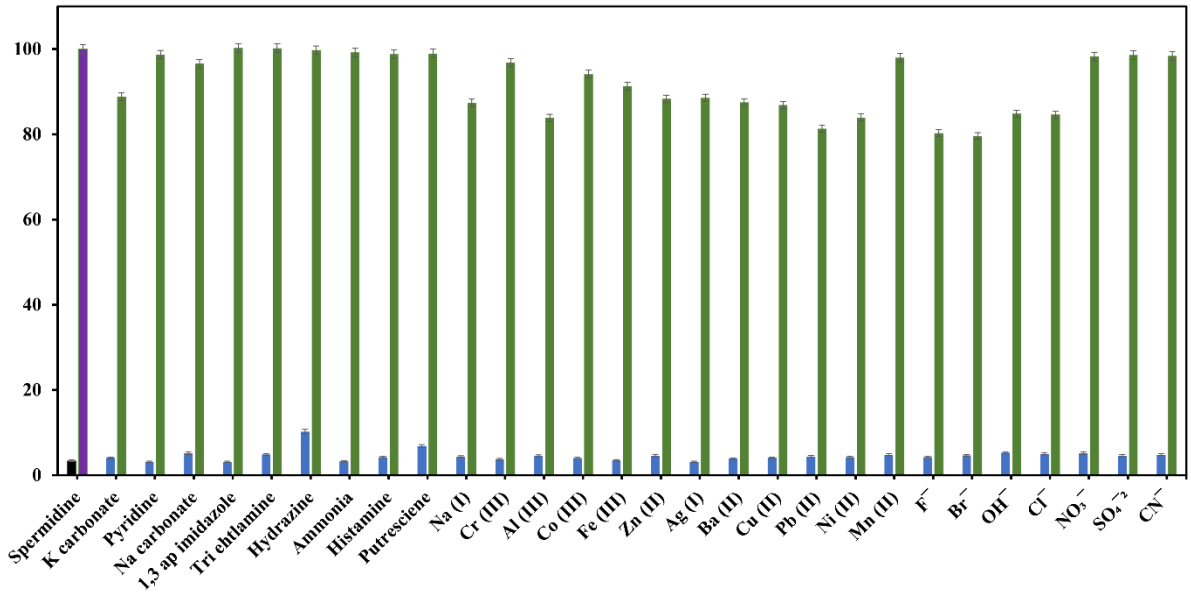

Fig S23 The % fluorescence intensity contrast bars to investigate the interference effect of other similar molecules and inorganic species to test objects on the detection ability of TP for Spermidine (SPD). TP-black, Purple-TP+SPD, Blue=TP+analytes, Green=TP+analytes+SPD

Table S1 Quantum Yield of the samples.

Sample	Integrated Emission	Abs at 365 nm	Refractive Index	Quantum Yield
Quinine Sulphate	12.19×E8	0.0622	1.33	54%(Known)
TP	2.65×E7	0.0189	1.33	3.7%
TP+SPM	5.67×E8	0.0214	1.33	73%
TP+SPD	5.00×E8	0.0233	1.33	58%
TPC	4.29×E7	0.0375	1.33	3.1%

Table S2 % recovery of analyte.

Sample (Water)	SPM (% Recovery)	SPD (% Recovery)	TP⊂SPM+HCHO (% Recovery)	TP⊂SPD+HCHO (% Recovery)
Drinking	72	74	91	94
Tap	48	50	91	92
Lake	58	56	76	84
River	79	83	79	67

Table S3 Comparison of some reported Spermine/ Spermidine receptors with the present work.

Sensor	Type	Solent System	Limit of Detection	Reference
novel dye 3-((7-hydroxy-4-methylcoumarin)methylene)aminophenylboronicacid in agarose gel	Turn On	Water	Spermine- 6μM Spermidine- 6μM	1
Terphenyl derivative with a crown ether moiety	Turn On	Water:Ethanol	Spermidine- 46nM	2
Cuprous iodide-based coordination polymers	Turn Off	Water	Spermine- 0.57μM Spermidine- 1.06μM	3
Anionic organic dye, Zincon (ONLY UV/VISIBLE STUDY)	Turn-ON	Water	Spermidine-30.7 nM Spermine- 25.1 nM	4
Tetraphenyl ethylene derivative	Turn On	CH_3CN:Water	Spermine- 0.70μM Spermidine- 1.17μM	5
Supramolecular assemblies R-SPM and NIR-SPM with SDS	Turn-ON	HEPES-SDS	Spermidine -77 nM Spermine-22 nM	6
6-bis(dimethylamino)-9-(ethylthio)xanthylium **(**PSE)	Colour change	Water	Spermine- 0.03 μM	7
2D halide perovskite	Turn OFF		7 ng mL−1 for spermidine	8
Eu based composite	Colour change	Aerogel	0.41 μmol/L for spermine	9
metal-mediated ethynylarene	Turn-ON	Water	Spermine – 25 μM	10
Naphthylamine-based	**Turn-ON**	**Water**	**Spermidine -15.29 nM** **Spermine-10.29 nM**	**Present Work**

References:

1. R. R. Nair, S. Debnath, S. Das, P. Wakchaure, B. Ganguly and P. B. Chatterjee, *ACS Appl. Bio Mater.*, 2019, **2**, 2374-2387.

2. R. Tejpal, M. Kumar and V. Bhalla, *Sens Actuators B.*, 2018, **258**, 841-849.

3. Z. Shi, Y. Wu, X. Zhang, Y. Gao, L. Qiao, Q. Hou and M. Wang, *Dyes Pigm*, 2023, **220**, 111659.

4. Y. Fukushima and S. Aikawa, *Tetrahedron lett.*, 2019, **60**, 151302.

5. M. Barros, S. Ceballos, P. Arroyo, J. A. Sáez, M. Parra, S. Gil, A. M. Costero and P. Gaviña, *Chemosensors*, 2021, **10**, 8.

6. N. Singla, S. Dhiman, M. Ahmad, S. Kaur, P. Singh and S. Kumar, *Sens. Diagn.*, 2024.

7. D. Wang, X. Ding, J. Xie, J. Wang, G. Li and X. Zhou, *Anal. Chim. Acta.*, 2024, **1285**, 342025.
8. T. T. Truong, H. B. Truong and Y.-I. Lee, *Anal.*, 2024, **149**, 2306-2316.

9. H. Chen, X. Dong, K. Ou, X. Cong, Y. Liao, Y. Yang and H. Wang, *Talanta*, 2025, ***282***, 126946.

10. J. T. Fletcher and B. S. Bruck, *Sens Actuators B. Chem*., 2015, 207, 843-848